Inorg. Chem. **2003**, *42*, 3609–3615

A Monovacant Heteropolytungstate Thioderivative: Synthesis and Characterization of $[(PW_{11}O_{39})_2(H_4Mo_4S_4O_6)]^{10-}$ and Related Isomers

Jérôme Marrot, Marie Anne Pilette, Francis Sécheresse, and Emmanuel Cadot*

Institut de Réactivité, Électrochimie et Microporosités, UMR CNRS 8637, Université de Versailles, 45 Avenue des France, 78035 Versailles Cedex, France

Received November 19, 2002

$[(PW_{11}O_{39})_2(Mo_4S_4O_4(OH_2)_2)]^{10-}$ anions were obtained through the stereospecific addition of the $[Mo_2S_2O_2]^{2+}$ oxothiocation to the monovacant α-$[PW_{11}O_{39}]^{7-}$ anion. $K_{10}[(PW_{11}O_{39})_2(Mo_4S_4O_4(OH_2)_2)]\cdot 25H_2O$ has been isolated as crystals and characterized by X-ray diffraction. The structure revealed a "sandwich-like" dimer of two α-$[PW_{11}O_{39}]^{7-}$ subunits assembled by the noteworthy central cluster $\{H_4Mo_4S_4O_6\}$. The crystallization of the crude product produces an isomerically pure compound, which was characterized by ^{31}P and ^{183}W NMR. IR data were also supplied. In solution, the compound isomerizes, giving a second diastereoisomer. A kinetic experiment, carried out by ^{31}P NMR, allowed the conditions of the thermodynamic equilibrium to be determined. A structural relationship between the two isomers is proposed, fully consistent with NMR data. Cisoid and transoid isomers result in the relative disposition of each $[PW_{11}O_{39}]^{7-}$ subunit, either staggered or eclipsed. An investigation of the formation of the $[Mo_2O_2S_2]^{2+}$ unit from the polycondensed cyclic precursor $[Mo_{10}S_{10}O_{10}(OH)_{10}(H_2O)_5]$ and the aggregation process resulting in the oxothio $[(PW_{11}O_{39})_2(Mo_4S_4O_4(OH_2)_2)]^{10-}$ compound has been undertaken. The studies were monitored by ^{31}P NMR and UV–vis spectroscopies. The reaction is quantitative in nearly stoichiometric conditions.

Introduction

Current activity in the chemistry of polyoxometalates is largely driven by potential applications in catalysis and medicine that require a continuous improvement of efficient and adapted molecular materials.[1] To this end, such a class of compounds offers the possibility to use polyvacant anions as primary building blocks to construct step-by-step, sophisticated, and well-designed multi-unit compounds. The method proved to be fruitful for giving compounds which have reached now the nanoscopic domain with original structures and unusual combinations of properties. Conversely, molybdenum−sulfur clusters are present in metallo-enzymes,[2] and the effect of sulfur-donor ligands on the chemistry of molybdenum is therefore of important interest.[3] On the basis that sulfur(−II) ions are generally invoked for stabilizing lower oxidation states (+V, +IV, and +III) of Mo or W atoms,[4] incorporation of S−Mo(W) clusters in the POM framework is expected to produce a new generation of polyoxometalates with modified electronic properties. Earlier works demonstrated that oxygen can be replaced by sulfur in POM architectures. In 1985, Klemperer and Schwartz introduced the first sulfur atom in a Linqvist anion and obtained the mixed oxo−thio compound $[W_5(NbS)O_{18}]^{3-}$.[5] The reaction was conducted by the use of adequate sulfuring reagent, the hexamethyldisilathiane $(CH_3)_3Si_2S$, which was revealed to be selective in the O−S substitution on the Nb atom. In a similar way, we extended this protocol to the α-$[PW_{11}NbO_{40}]^{4-}$ heteropolyanion and characterized the {Nb═S}-introduced group in the Keggin anion.[6] Then, we developed another route of synthesis for sulfur-containing polymetalates. In 1996, we isolated the γ-$[SiW_{10}M_2S_2O_{38}]^{6-}$ by reacting the thiocationic core $[M_2O_2S_2]^{2+}$ with the divacant γ-$[SiW_{10}O_{36}]^{8-}$ anion.[7] The key to the method was

* Author to whom correspondence should be addressed. E-mail: cadot@chimie.uvsq.fr. Fax: (+33) 1 39 25 43 81.

(1) (a) See for example the special issues on polyoxometalates in *Chem. Rev.* **1998**, *98*(8) and *C. R. Acad. Sci. Paris, Ser. IIc*, **1998**. (b) *Polyoxometalates: From Platonic Solids to Anti-Retroviral Activity*; Pope, M. T., Müller, A., Eds.; Kluwer: Dordrecht, The Netherlands, 1994.
(2) (a) Spiro, T. G., Ed. *Molybdenum Enzymes*; Wiley: New York, 1985. (b) Stiefel, E. I., Coucouvanis, D., Newton, W. E., Eds. *Molybdenum Enzymes, Cofactors and Model Systems*, ACS Symposium Series 535; American Chemical Society: Washington, DC, 1993.
(3) Coucouvanis, D. *Adv. Inorg. Chem.* **1997**, *45*, 1.
(4) Shibahara, T. *Coord. Chem. Rev.* **1993**, *123*, 73−147.
(5) Klemperer, W. G.; Schwartz, C. *Inorg. Chem.* **1985**, *24*, 4459.
(6) Cadot, E.; Béreau, V.; Sécheresse, F. *Inorg. Chim. Acta* **1995**, *239*, 39.
(7) Cadot, E.; Béreau, V.; Halut, S.; Sécheresse, F. *Inorg. Chem.* **1996**, *35*, 551.

10.1021/ic026191j CCC: $25.00
Published on Web 05/09/2003

found from a work of Coucouvanis et al., who reported on an elegant way to produce selectively and quantitatively the $[Mo_2O_2S_2]^{2+}$ oxothiocation.[8] We extended the Coucouvanis reaction scheme to the tungsten analogue $[W_2O_2S_2]^{2+}$.[7] Thus, we characterized the "sandwich-type" compound $[(PW_9O_{34})_2(M_2O_2S_2(H_2O)_2)_3]^{12-}$ in which the three oxothiometallic cores $\{M_2S_2O_2\}$ act as linkers between the trivacant α-$[PW_9O_{34}]^{9-}$ subunits,[9] whereas Müller et al. gave an example of the conversion of $[Mo_3S_4(H_2O)_9]^{4+}$ into the nanosized cluster complexes $[[(SiW_{11}O_{39})Mo_3S_4(H_2O)_3(\mu\text{-}OH)]_2]^{10-}$ and $[[(P_2W_{17}O_{61})Mo_3S_4(H_2O)_3(\mu\text{-}OH)]_2]^{14-}$ by reaction with $[SiW_{11}O_{39}]^{8-}$ and $[P_2W_{17}O_{61}]^{10-}$, respectively.[10] Regarding the potentialities of the method and the growth of interest for such compounds, this field of investigations continues to be one of our main focuses. We present herein the synthesis and characterization of the oxo−thio heteropolyanions, obtained from direct addition of the dication $[Mo_2O_2S_2]^{2+}$ on the monovacant polyanion α-$[PW_{11}O_{39}]^{7-}$.

Experimental Section

Synthesis. All chemicals were commercially available reagent-grade quality and used as received. The cyclic precursor (**1**) was prepared by the synthetic procedure described in ref 11. The previous characterization[12,13] of this crude compound led to the composition $K_2I_2[Mo_{10}S_{10}O_{10}(OH)_{10}(H_2O)_5]\cdot 15H_2O\cdot\epsilon NMe_4N$ according to the elemental analysis: calcd (found) K, 3.50 (3.55); I, 10.87 (11.03); Mo, 40.77 (40.80); S, 13.59 (13.71). The monovacant heteropolytungstate α-$K_7PW_{11}O_{39}\cdot 14H_2O$ was prepared according to the procedure described by Contant.[14]

$\Delta_{1,2}$-$K_{10}[(PW_{11}O_{39})_2(Mo_4S_4O_4(OH_2)_2)]\cdot 20H_2O$. $K_2I_2[Mo_{10}S_{10}O_{10}(OH)_{10}(H_2O)_5]\cdot 15H_2O\cdot\epsilon NMe_4$ (**1**) (3.15 g; 1.28 mmol) was suspended in 100 mL of water with 4 mL of 4 mol·L^{-1} HCl. Then $K_7PW_{11}O_{39}\bullet 14H_2O$ (19.0 g; 5.93 mmol) was poured into the solution under vigorous stirring. The color of the solution quickly turned from yellow to deep red-brown. After 30 min, potassium chloride (22 g; 295.1 mmol) was added, provoking the precipitation of the brown potassium salt **$K_{10}[(PW_{11}O_{39})_2(Mo_4S_4O_4(OH_2)_2)]\cdot 20H_2O$.** After 12 h under slow stirring, the solid was collected by filtration, washed, and dried with ethanol and diethyl ether to give 19.7 g of a brown powder (95% yield based on W). The crude product was a mixture of two isomers, noted Δ_1 and Δ_2. Anal. Calcd (found) for $K_{10}[(PW_{11}O_{39})_2(Mo_4S_4O_4(OH_2)_2)]\cdot 20H_2O$: K, 5.82 (5.55); W, 60.02 (60.05); Mo, 5.71 (5.76); S 1.91(1.93). ^{31}P NMR in D_2O-H_2O (1:1) showed two peaks at $\delta(\Delta_1) = -10.95$ ppm and $\delta(\Delta_2) = -10.86$ ppm with a 25:75 intensity ratio. FTIR: $\bar{\nu}$[cm^{-1}]: 1096(m), 1035(sh), 973(sh), 950(s), 891(m), 853(s), 775(s), 690(vw), 597(vw), 579(vw), 515(w), 469(vw), 367(m), 328(m).

Δ_1-$K_{10}[(PW_{11}O_{39})_2(Mo_4S_4O_4(OH_2)_2)]\cdot 20H_2O$. The crude product $\Delta_{1,2}$-$K_{10}[(PW_{11}O_{39})_2(Mo_4S_4O_4(OH_2)_2)]\cdot 20H_2O$ (10.0 g; 1.48 mmol) was dissolved in 300 mL of a 1 mol·L^{-1} KCl aqueous solution. The isomerically pure compound Δ_1-$K_{10}[(PW_{11}O_{39})_2(Mo_4S_4O_4(OH_2)_2)]\cdot 20H_2O$ selectively crystallized from the isomer mixture. The resulting filtrate was allowed to stand at room temperature. A week was required for the growth of well-shaped parallelepiped crystals suitable for the X-ray diffraction experiment. Δ_1 compound was obtained (8.0 g), with 80% yield based on $[(PW_{11}O_{39})_2(Mo_4S_4O_4(OH_2)_2)]^{10-}$. Crystals were strongly unstable in ambient air and rapidly lost five water molecules of crystallization: 25 water molecules were located by the X-ray diffraction study in the glass tube-stabilized crystal and 20 by the TGA experiment on the air-stable hydrate.

^{31}P NMR in D_2O-H_2O (1:1) showed a main peak at $\delta(\Delta_1) = -10.95$ ppm, but as the isomerization reaction took place, the profile of the second peak Δ_2 grew from the background (less 5% after 5 min at room temperature).

Elemental analysis was performed by the Service Central d'Analyses du CNRS. The water content was determined by thermal gravimetric analysis (TGA experiments) with a TGA7-Perkin-Elmer apparatus.

Infrared spectra were recorded on an IRFT Magna 550 Nicolet spectrophotometer using the technique of pressed KBr pellets.

^{183}W NMR spectra were recorded at 20 °C from a saturated solution in polyanion (Li^+ salt) on a Bruker AC-300 spectrometer operating at 12.5 MHz in 10-mm tubes. Chemical shifts were referenced to an external 2 mol·L^{-1} Na_2WO_4 solution in alkaline D_2O and to the α-dodecatungstosilicic acid as secondary standard ($\delta = -103.8$ ppm). The saturated aqueous solution of $Li_{10}[(PW_{11}O_{39})_2(Mo_4S_4O_4(OH_2)_2)]$ was obtained by cationic exchange of the corresponding potassium salt through a Dowex 50W-X2 resin (Li^+ form). The eluate was evaporated until dry and dissolved in a mixture of H_2O-D_2O (v/v) to obtain a concentration of about 0.8 M.

^{31}P NMR spectra were recorded at the nominal frequency of 121.5 MHz. Spectra were referenced to external 85% H_3PO_4 in 5-mm tubes.

UV−vis spectra were recorded at room temperature with a Perkin-Elmer Lambda 19 spectrophotometer using 0.1-cm quartz crystal cells. The formation of the aqua ion $[(H_2O)_6Mo_2O_2S_2]^{2+}$ from the polycondensed ring $[Mo_{10}S_{10}O_{10}(OH)_{10}(H_2O)_5]$ was studied at constant ionic strength, imposed by a 0.05 mol·L^{-1} NaCl concentration.

X-ray Crystallography. A well-shaped red-brown crystal (0.40 × 0.40 × 0.3 mm^3) of $K_{10}[(PW_{11}O_{39})_2(Mo_4S_4O_4(OH_2)_2)]\cdot 25H_2O$ was mounted in a Lindemann tube for indexing and intensity data collection at room temperature on a Siemens SMART-CCD area detector system equipped with a normal-focus, molybdenum-target X-ray tube ($\lambda = 0.71073$ Å). Intensity data were collected in 1271 frames with increasing ω (width of 0.3° per frame). Unit cell dimensions were refined by a least-squares fit on reflections. Of the 19 197 reflections, 13 275 unique reflections ($R_{int} = 0.0531$) and 9695 were considered ($I > 2\sigma(I)$). Corrections for polarization and Lorentz effects were applied. An absorption correction was performed using the SADABS program[15] based on the methods of Blessing.[16] Direct methods were used to locate the heaviest atoms, and then sulfur, potassium phosphorus, and oxygen atoms were found from successive refinements by full-matrix least-squares using the SHELX-TL package.[17] The final refinement cycle including the atomic coordinates, anisotropic thermal parameters (atoms of the heteropolyanion), and isotropic thermal parameters (for the K^+

(8) Coucouvanis, D.; Toupadakis, A.; Hadjikyriacou, A. *Inorg. Chem.* **1988**, *27*, 3272.
(9) Béreau, V.; Cadot, E.; Bögge H.; Müller A.; Sécheresse, F. *Inorg. Chem.* **1996**, *38*, 551.
(10) Müller, A.; Fedin, V. P.; Khulmann, C.; Fenske, H. D.; Baum, G.; Bögge, H.; Hauptfleisch, B. *Chem. Commun.* **1999**, 1189.
(11) Cadot, E.; Salignac, B.; Halut, S.; Sécheresse, F. *Angew. Chem., Int. Ed.* **1998**, *37*, 611−612.
(12) Cadot, E.; Salignac, B.; Marrot, J.; Dolbecq, A.; Sécheresse, F. *Chem. Commun.* **2000**, 261−262.
(13) Cadot, E.; Salignac, B.; Dolbecq, A.; Sécheresse, *J. Phys. Chem. Solids* **2001**, *62*, 1533.
(14) Contant, R. *Can. J. Chem.* **1987**, *65*, 568.
(15) Sheldrick, G. M. *SADABS*; Program for scaling and correction of area detector data; University of Göttingen, Germany, 1997.
(16) Blessing, R. *Acta Crystallogr.* **1995**, *A51*, 33.

Table 1. Crystallographic Data for $K_{10}[(PW_{11}O_{39})_2(Mo_4S_4O_4(OH_2)_2)]\cdot 25H_2O$

formula	$K_{10}[(PW_{11}O_{39})_2(Mo_4S_4O_4(OH_2)_2)]\cdot 25H_2O$
M_r [g mol^{-1}]	6753.64
color	brown
cryst dimension [mm]	0.40 × 0.40 × 0.30
cryst syst	triclinic
space group	$P\bar{1}$
T [K]	298
a [Å]	11.6764(1)
b [Å]	13.5414(2)
c [Å]	19.9173(3)
α [°]	84.302(1)
β [°]	81.514(1)
γ [°]	64.484(1)
V [Å^3]	2808.7(5)
Z	1
ρ_{calc} [g cm^{-3}]	3.993
μ [mm^{-1}]	23.434
θ range [°]	1.03−28.00
reflns measured	19 197
unique reflns (R_{int})	13 275(0.0531)
observed ($I > 2\sigma(I)$)	9695
refined params	677
$R_1(F)^a$	0.0599
w$R_2(F^2)^b$	0.1524
$\Delta\rho$(max/min) [e Å^{-3}]	4.224/−2.349

^{a} $R_1 = (\sum||F_o| - |F_c||)/\sum|F_c|$. ^{b} w$R_2 = (\sum w(F_o^2 - F_c^2)^2)/\sum w(F_o^2)^2$, with $1/w = \sigma^2F_o^2 + (aP)^2 + bP$, $P = (F_o^2 + 2F_c^2)/3$, $a = 0.0801$, and $b = 0$.

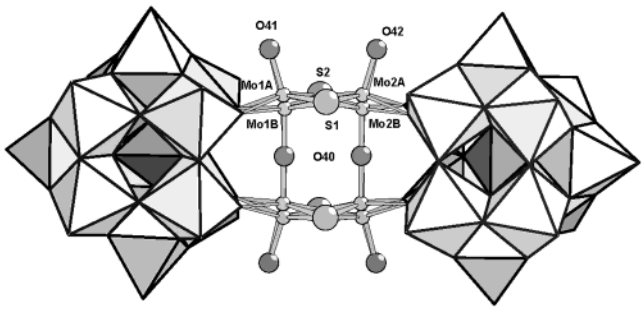

Figure 1. Perspective view of the transoid anion (Δ_1 isomer) $[(PW_{11}O_{39})_2(Mo_4S_4O_4(OH_2)_2)]^{10-}$. The central cluster $\{H_4Mo_4S_4O_6\}$ is represented in the ball-and-stick model, whereas a coordination polyhedra representation is used for the two $\{PW_{11}\}$. The two distinct Mo1 and Mo2 atoms are disordered over two positions labeled A (outer) and B (inner).

cations and oxygen atoms of crystallization water molecules) converged toward $R_1 = 0.0599$, w$R_2 = 0.1524$. Crystallographic data are given in Table 1. The anion with selected labeled atoms is shown in Figure 1. Selected bonds and angles are given in Table 2.

Results and Discussion

Molecular Structure of Δ_1-$[(PW_{11}O_{39})_2(Mo_4S_4O_4(OH_2)_2)]^{10-}$. In the Solid State. The molecular representation of the structure given in Figure 1 reveals a dimeric association of two α-$[PW_{11}O_{39}]^{7-}$ units sandwiching two oxothio-fragments. The two $\{Mo_2O_2S_2\}$ entities are blocked in the center of the molecule and are directly and symmetrically bonded to the four terminal oxygen atoms, delimiting the vacancy of each α-$[PW_{11}]$ subunit. In this arrangement, the α-$[PW_{11}]$ subunits act as bis-bidentate ligands, constraining

Table 2. Selected Bond Lengths [Å] for $[(PW_{11}O_{39})_2(Mo_4S_4O_4(OH_2)_2)]^{10-}$

	bond lengths [Å]	average [Å]
	$\{PW_{11}\}$ subunit	
W═O	1.674(14)−1.709(15)	1.697
W−O(W)	1.806(12)−2.041(12)	1.915
W−O(Mo)	1.761(9)−1.773(10)	1.757
W−O(P)	2.327(11)−2.496(9)	2.406
P−O	1.527(10)−1.540(11)	1.534
	$\{H_4Mo_4S_4O_6\}$ core	
MoA═O	1.685(15)−1.696(16)	1.690
MoA−O(MoB)	2.201(15)−2.204(14)	2.202
MoB═O(MoA)	1.701(14)−1.687(14)	1.694
MoB−OH_2	2.176(15)−2.204(16)	2.196
Mo−S	2.290(6)−2.317(6)	2.294
Mo−O(W)	2.025(14)−2.147(12)	2.075
Mo−Mo		
syn	2.824(8)−2.772(8)	2.798
anti	2.841(8)−2.847(8)	2.844

	angles [°]	average [°]
	Mo−S−Mo	
syn	74.6(3)−77.0(3)	75.2
anti	76.3(3)−76.9(3)	76.6

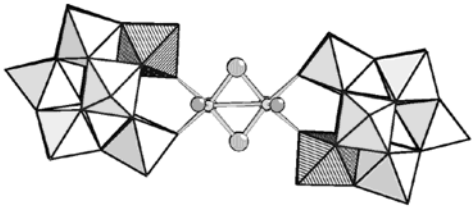

Figure 2. Highlighted transoid arrangement: The two equivalent hatched octahedra clearly show the 180°-staggered conformation of the two $\{PW_{11}\}$ subunits.

the two $\{Mo_2O_2S_2\}$ moieties to interact through a quasi-linear double Mo−O−Mo bridge. An inversion center generates the dimeric anion from the asymmetric unit. In the resulting compound, the two α-$\{PW_{11}\}$ subunits have no local symmetry and have relative 180°-staggered conformations (Figure 2). According to the terminology proposed by Pope et al. for uranyl-containing complexes, the Δ_1 compound corresponds to a transoid isomer.[18] The two Mo atoms of the asymmetric unit are symmetrically placed *over*, rather than *in* the vacancy site in each α-$[PW_{11}]$. A similar association has been previously reported by Finke et al. in the structure of the "$(P_2W_{17}Ru)_2$−O" dimer.[19] In the former compound, the two monovacant heteropolyanions α-$[P_2W_{17}]^{10-}$ are attached to a central $\{Cl-Ru-O-Ru-Cl\}^{4+}$ cluster (instead of $\{H_4Mo_4S_4O_6\}^{4+}$), in a transoid fashion. Another example is the "sandwich-like" compound $[SiW_{11}Mo_3S_4(OH_2)_3(OH)]_2$.[10] The central cationic cluster results from the bridging of two $\{Mo_3S_4\}^{4+}$ clusters by a double hydroxo junction, whereas the two hanging α-$[SiW_{11}]^{8-}$ units are in an "eclipsed" arrangement to give a cisoid isomer. In the Δ_1 compound, the two molybdenum atoms Mo1 and Mo2 are equally distributed over two positions, labeled A and B for outer and inner Mo, respectively. Such a disorder induces some ambiguity in the complete description of the structure,

(17) (a) Sheldrick, G. M. *Acta Crystallogr*. **1990**, *A46*, 467. (b) Sheldrick, G. M. *SHELX-TL*, version 5.03; Software Package for the Crystal Structure Determination; Siemens Analytical X-ray Instrument Division: Madison, WI, 1994.

(18) Termes, S. C.; Pope, M. T. *Transition Met. Chem*. **1978**, *3*, 103.

(19) Randall, W. T.; Weakley T. J. R.; Finke, R. G. *Inorg. Chem*. **1993**, *32*, 1068.

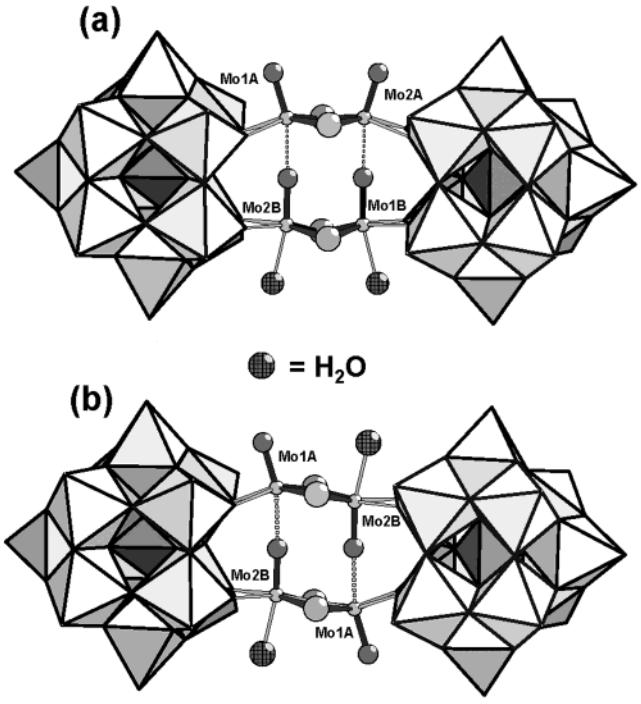

Figure 3. Perspective view of the two possible arrangements for the transoid anion in agreement with NMR data: (a) C_i symmetry structure containing a syn−syn conformation in the $\{H_4Mo_4S_4O_6\}$ central core; (b) C_2 symmetry structure exhibiting an anti−anti conformation for the $\{H_4Mo_4S_4O_6\}$ central core.

which requires the location of four protons, necessarily distributed over the six oxygen atoms of the central $\{Mo_4S_4O_6\}$ cluster. Bond valence sum (BVS) calculations clearly agree with two unprotonated Keggin units. Conversely, the presence of two aquo ligands, each bonded to Mo1B and Mo2B, fully confirms the BVS calculations.[20,21] In fact, the disorder of the Mo atoms generates two distinct distances for terminal Mo−O bonds: the long MoB−O distances [2.176(15)−2.204(16) Å] reflect the presence of terminal aquo ligands, whereas the shortest MoA−O distances [1.685(15)−1.696(16) Å] are characteristic of terminal oxo groups. At this point, the location of the two terminal aquo ligands is ambiguous because several possibilities exist to distribute the $Mo-OH_2$ groups within the central $\{Mo_4S_4O_6\}$ cluster. Therefore, only the two possibilities depicted in Figure 3, showing C_2 and C_i symmetry are in agreement with ^{31}P and ^{183}W NMR characterizations (see below). The C_2 symmetry involves two syn dimers (Figure 3a), whereas for the C_i possibility, the two $\{Mo_2S_2O_2\}$ cores have the anti stereochemistry (Figure 3b). In the C_2 solution, the disorder results in the statistical distribution of two enantiomers over a single position to give a racemic mixture in the crystal. In the C_i option, the disorder is due to a statistical stacking of the anion. At this stage, the data agree with the two possibilities, and no definitive conclusion can

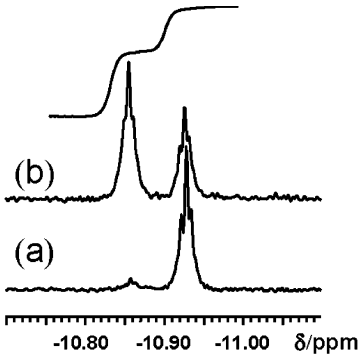

Figure 4. ^{31}P NMR spectra: (a) pure Δ_1 isomer (transoid) after 5 min in solution at 25 °C; (b) mixture of Δ_1 (transoid) and Δ_2 (cisoid) at equilibrium (the multiplet patterns are due to the $^2J_{P-O-W}$ coupling expected in the 1−2 Hz range).

be formulated upon the geometry of the central core $\{H_4Mo_4S_4O_6\}^{4+}$. The μ-disulfido-bridged dinuclear molybdenum(V) has been observed in both syn and anti stereochemistries,[22,23] and here, the geometrical data, bond lengths, and angles are compatible with both the geometries (Table 2). The bonding scheme in the syn and anti isomers of the $\{Mo_2S_4\}^{2+}$ core was theoretically studied, and calculations using extended Hückel and Fenske−Hall approaches indicated that the syn isomer is the most stable.[24] It should be noted that the anti isomer has been exclusively obtained in anhydrous solvent as CH_3CN. A rational synthesis of the anti core has been previously reported by Coucouvanis et al.[23] The starting material used was the $[Mo_2O_2S_9]^{2-}$ anion, which permits a free rotation of the two {Mo═O} moieties along the Mo−S−Mo bridges,[25] producing in CH_3CN solution the two syn and anti isomers. The conversion of the anti into the syn conformation is H_3O^+-catalyzed, and thus the presence of the anti conformation in water-containing solvent is likely not expected.[23] These features rather argue for a syn−syn interaction, depicted in Figure 3a, without any change in the syn conformation of the dinuclear cores during the assembling process. Ultimately, the definitive conclusion for this unusual cluster $\{H_4Mo_4S_4O_6\}^{4+}$ should require theoretical calculations to deduce the most stable conformation.

NMR Characterizations in Solution. The ^{31}P NMR spectrum of the Δ_1-$[(PW_{11}O_{39})_2(Mo_4S_4O_4(OH_2)_2)]^{10-}$, given in Figure 4, consists of a single line (−10.95 ppm) showing that the two $\{PW_{11}\}$ subunits of the dimer are equivalent and in agreement with the single-crystal X-ray diffraction study. Therefore, the ^{31}P NMR spectrum is time dependent because the −10.95 ppm line, assigned to the Δ_1 compound, gradually decreases to give a second line at −10.86 ppm, attributed to the Δ_2 compound (Figure 4). The kinetic of the conversion process was monitored by ^{31}P NMR at 60 °C and is graphically shown in Figure 5. The chemical system

(20) The BVS are calculated according to ref 21. For an unprotonated oxygen atom, the BVS results fall between a range of −2.2 and −1.8, whereas the diprotonated O41 and O42 have values of −0.45 and −0.48, respectively.

(21) (a) Brown, I. D.; Altermatt D. *Acta Crystallogr*. **1985**, *B41*, 244−247. (b) Brese, N. E.; O'Keefe, M. *Acta Crystallogr*. **1991**, *B47*, 192−197.

(22) Bunzey G.; Henemark, J. H.; Howie, J. K.; Sawyer, D. T. *J. Am. Chem. Soc.* **1977**. *99*, 4168.

(23) Coucouvanis, D.; Hadjikyriacou, A. I.; Toupadakis, A.; Koo, S.-M.; Ileperuma, O.; Draganjac, M.; Salifoglou, A. *Inorg. Chem.* **1991**, *30*, 754.

(24) Chandler, T.; Lichtenberger, D. L.; Enemark, J. H. *Inorg. Chem*. **1981**, *20*, 75.

(25) Hadjikyriacou, A. I.; Coucouvanis, D. *Inorg. Chem*. **1989**, *28*, 2169.

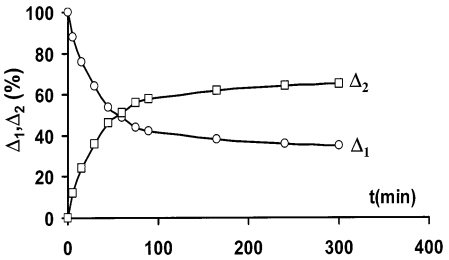

Figure 5. Kinetic plots of the isomerization process of the Δ_1 into the Δ_2 isomer at 60 °C.

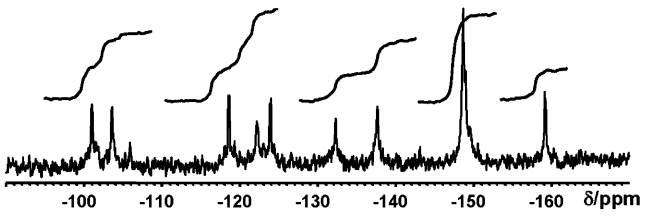

Figure 6. ^{183}W NMR spectrum of the Δ_1 isomer (0.4 mol·L^{-1} at 23 °C) after 2 h of acquisition.

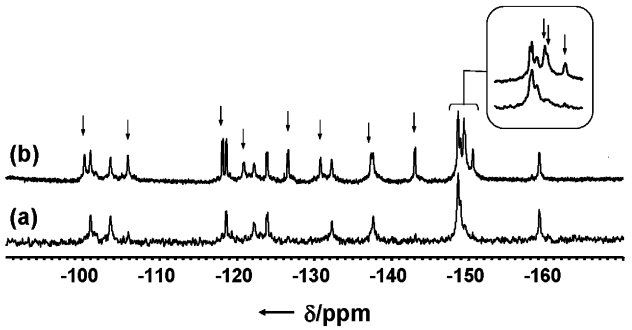

Figure 7. ^{183}W NMR spectra of the Δ_1 isomer (a) after 2 h and (b) after 48 h. Arrows highlight the 11 additional lines of the Δ_2 compound.

reaches an equilibrium state after about 2 h at 60 °C, characterized by a 2:1 intensity ratio for the Δ_2 and Δ_1 (transoid) resonance lines, respectively. The close chemical shifts related to the two resonances ($\Delta\delta \approx 0.1$ ppm) and the possibility to regenerate Δ_1 from the 2:1 mixture in quantitative yield by crystallization are good arguments to state that both Δ_2 and Δ_1 are related through an isomerization process.

The ^{183}W NMR spectrum of the Δ_1 isomer, shown in Figure 6, consists of 11 equal resonances attributed to the 11 tungsten atoms involved in the α-$[PW_{11}O_{39}]^{7-}$ subunit with no symmetry. Eight peaks are well-resolved, whereas three resonances overlap at about −150 ppm, giving an asymmetric pattern. This result confirms that the lack of symmetry, yet observed in the solid state for the two $\{PW_{11}\}$ moieties, is maintained even in solution. These 11 resonances, observed between −100 and −160 ppm, have the usual values reported for octahedral tungsten(VI) atoms in an oxide−ions environment. As previously evidenced by ^{31}P NMR, the ^{183}W NMR spectrum changes with time to show 11 additional lines, characteristic of the Δ_2 compound (Figure 7). Finally, the resulting ^{183}W NMR spectrum exhibits two sets of 11 lines as expected for the isomerization of Δ_1 into Δ_2. At the equilibrium, the relative intensities of the ^{183}W signals are in agreement with a 1/3−2/3 proportion for Δ_1 and Δ_2, respectively. The two $\{PW_{11}\}$ subunits are equivalent

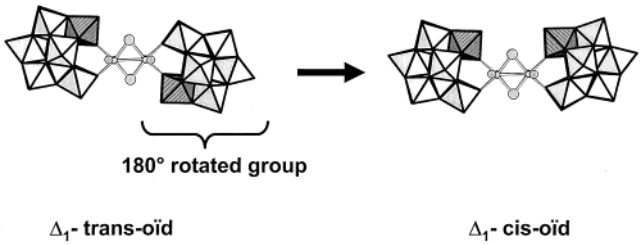

Figure 8. Relationship between the transoid and cisoid arrangements in $[(PW_{11}O_{39})_2(Mo_4S_4O_4(OH_2)_2)]^{10-}$.

and exhibit no local symmetry in the Δ_1 (transoid) as well as in the Δ_2 arrangements. ^{183}W NMR data of the Δ_1 and Δ_2 isomers are reported in Table 3.

Relationship between the Δ_1 and Δ_2 Arrangements. The very close ^{31}P and ^{183}W NMR features and the possibility to convert reversibly and reciprocally Δ_1 into Δ_2 argue for an isomeric system. Actually, the Δ_1 arrangement, which has been structurally characterized by single-crystal X-ray crystallography, can provide naturally one isomer through the rotation of one $\{PW_{11}\}$ subunit of 180° with respect to the other two, to give the cisoid isomer, as depicted in Figure 8. In the two isomers, Δ_2 and Δ_1, the two $\{PW_{11}\}$ subunits exhibit exactly the same mode of connection within the central tetranuclear core. In the Δ_2 (cisoid) isomer, the two $\{PW_{11}\}$ are equivalent and exhibit no local symmetry, according to the observed single ^{31}P line and the 11 ^{183}W resonances. At this point, the determination of the symmetry of the anion remains ambiguous and depends on the location of the two aquo ligands to give a syn−syn or anti−anti interaction within the central core. Despite the long distance observed between the two $\{PW_{11}\}$ (about 12 Å), making them nearly independent, a slight but significant contribution of the relative orientations of the $\{PW_{11}\}$ subunit to the stability of the isomer is observed. At the equilibrium, the distribution corresponds to a Δ_2/Δ_1 ratio equal to 2, signifying an increasing stability for the cisoid arrangement. The long distance between the two $\{PW_{11}\}$ polyanions, which can be viewed as spherical bulks, prevents any mutual steric influence but rather argues for an electronic effect such as a trans influence, spread along the Mo−S bonds. The origin of such an effect likely arises from the difference of the basicity of the oxygen atoms surrounding the vacancy of the $\{PW_{11}\}$ polyanion. The facile isomerization of the transoid species is due to the lability of the Mo−O bonds involved in the Mo−O−W junctions. The Mo−O bond lengths [2.025(14)−2.147(12) Å] are substantially longer than the W−O bonds [1.761(9)−1.773(10) Å], which have partly retained the double bond character as in the parent α-$[PW_{11}O_{39}]^{7-}$ (see Table 2). Thus, the dimeric association can be viewed as a labile complex where the two bulky α-$[PW_{11}]$ units have the possibility to wheel around an axis passing through the central $\{H_4Mo_4S_4O_6\}^{4+}$ cluster (see Figure 8).

Synthesis. Hydrolysis of the Thioprecursor. We report here on a straightforward procedure to generate readily a solution of oxothiocation. The method consists of an acidic hydrolysis of the cyclic precursor $\{K_2(N(CH_3)_4)_{0.75}I_{2.75}$-

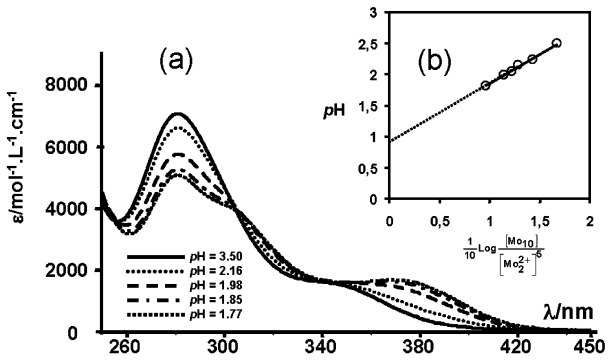

Figure 9. (a) UV−vis spectra of $\{Mo_2O_2S_2\}$-containing solutions at various pH. (b) Graphical treatment of the data according to the proposed equilibrium: $[Mo_{10}] + 10H^+ \rightleftharpoons 5[Mo]^{2+}$.

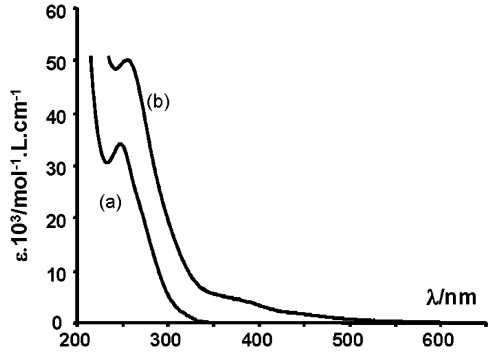

Figure 10. UV−vis spectrum of (a) the monovacant precursor α-$[PW_{11}O_{39}]^{7-}$ and (b) the red-brown product $\Delta_{1,2}$-$[(PW_{11}O_{39})_2(Mo_4S_4O_4(OH)_2]^{10-}$.

$[Mo_{10}S_{10}O_{10}(OH)_{10}(H_2O)_5]\}\cdot 15H_2O$ (**1**) to give the reactive $[Mo_2S_2O_2]^{2+}$ thiofragment. The precursor (**1**) was synthesized through a selective oxidation process of the dianionic primary precursor $[Mo_2O_2S_6]^{2-}$, followed by a basic treatment which isolates the $\{Mo_2O_2S_2\}$ fragment under a polycondensed form. The neutral $[Mo_{10}S_{10}O_{10}(OH)_{10}(H_2O)_5]$ molecule, noted $[Mo_{10}]$, was extracted from solution as a bis-iodide complex, $\{I_2Mo_{10}]^{2-}$, which has been structurally characterized by single-crystal X-ray diffraction through recrystallization of **1** in DMF medium. The behavior of the $[Mo_{10}]$ ring in varying acidity was followed by UV−vis spectrometry; selected spectra of solutions of 0.00182 mol·L^{-1} in $[Mo_2]$ dimer are shown in Figure 9, and UV−vis spectroscopic data are presented in Table 4. The acidification of a $[Mo_{10}]$ solution, from pH 3.5 to 1.70, brings significant changes in the UV−vis features. In the 260−450 nm region, the presence of two isosbestic points for three main absorptions (maxima and shoulder) seems to be in agreement with an equilibrium involving only two absorbing compounds. At pH below 1.80, the UV−vis spectrum exhibits the characteristics of the aqua ion $[(H_2O)_6Mo_2O_2S_2]^{2+}$ in good agreement with those reported in the literature.[26,27] Then, the equilibrium related to the changes of the UV−vis absorptions can be expressed as eq 1.

$$[Mo_{10}] + 10H^+ \rightleftharpoons 5\,[Mo_2]^{2+} \qquad (1)$$

The fraction of dimer under cationic form (x) is extracted from the molar extinction coefficient ϵ of the mixture, expressed by eq 2, where ϵ_1 (5163 mol^{-1}·L·cm^{-1}) and ϵ_2 (7370 mol^{-1}·L·cm^{-1}) are the molar extinction coefficients per dimer of $[Mo_2^{2+}]$ and $[Mo_{10}]$, respectively (see Table 4).

$$\epsilon = x(\epsilon_1 - \epsilon_2) + \epsilon_2 \qquad (2)$$

The concentrations in $[Mo_2^{2+}]$ and $[Mo_{10}]$ at the equilibrium are deduced from the x values and the global concentration in dimer and then used for the calculation of the equilibrium constant (eq 3).

$$K = \frac{[Mo_{10}][H^+]^{10}}{[Mo_2^{2+}]^5} \qquad (3)$$

The various experimental absorptions obtained from the ϵ values at 280 nm give a set of reliable data in agreement with the linear expression deduced from the logarithmic conversion of (3). A graphical treatment (Figure 9b) gives pK = 8.9.

Formation of $\Delta_{1,2}$-$[(PW_{11}O_{39})_2(Mo_4S_4O_4(OH_2)_2)]^{10-}$. The UV−vis spectra of the parent α-$[PW_{11}O_{39}]^{7-}$ (noted α-$[PW_{11}]$) and the thioderivative $\Delta_{1,2}[(PW_{11}O_{39})_2(Mo_4S_4O_4(OH_2)_2)]^{10-}$ (noted $[PW_{11}Mo_2]$) are shown in Figure 10. The first experiment studies solutions with a fixed $[PW_{11}]$/[dimer] ratio of 1 by varying the pH. The concentration in $[PW_{11}Mo_2]$ is determined by measuring the absorbance at 440 nm (ϵ = 2222 mol^{-1}·L·cm^{-1} per dimer). Absorptions in the 420−500 nm range are characteristic of the red-brown thioderivatives $\Delta_{1,2}$-$[(PW_{11}O_{39})_2(Mo_4S_4O_4(OH_2)_2)]^{10-}$ because $[Mo_{10}]$, $[Mo_2]^{2+}$, and $[PW_{11}]$ do not exhibit significant absorptions in this region. The formation of $[PW_{11}Mo_2]$ versus the H^+ quantity per dimer is graphically shown in Figure 11a. The results reveal that at pH = 2.9 (3.5 H^+ per dimer), about 80% of the monovacant $[PW_{11}]$ is converted into $[PW_{11}Mo_2]$ thioderivatives. At lower pH, decomposition of $[PW_{11}O_{39}]^{7-}$ into $[PW_{12}]^{3-}$ is observed, which decreases the yield of the expected compound $\Delta_{1,2}$-$[(PW_{11}O_{39})_2(Mo_4S_4O_4(OH_2)_2)]^{10-}$. The second experiment (Figure 11b) confirms the 1:1 stoichiometry of the complex and reveals that a quasi-stoichiometric ratio H^+/dimer leads to a total conversion of the precursors into the $\Delta_{1,2}$-$[(PW_{11}O_{39})_2(Mo_4S_4O_4(OH_2)_2)]^{10-}$ product. The spectral titrations of a $[Mo_{10}]$ solution containing 4 H^+ per dimer by $[PW_{11}O_{39}]^{7-}$ are graphically shown in Figure 11b. A break point is observed in the curve at $[PW_{11}O_{39}]^{7-}$/dimer = 1, confirming the complete conversion of the precursors in stoichiometric conditions. Such a result is supported by the ^{31}P NMR titration of a solution of $[PW_{11}]$ by an acidified solution of $[Mo_{10}]$ (Figure 11c). Overall ^{31}P NMR spectra show that α-$[PW_{11}O_{39}]^{7-}$ (δ = −10.6 ppm) is selectively converted into the two expected isomers $\Delta_{1,2}$-$[(PW_{11}O_{39})_2(Mo_4S_4O_4(OH_2)_2)]^{10-}$ ($\delta(\Delta_1)$ = −10.95 ppm and $\delta(\Delta_2)$ = −10.86 ppm). The addition of the oxothiocation to the monovacant polyoxoanion is rapid and generates spon-

(26) Armstrong, F. A.; Shibahara, T.; Sykes, A. G. *Inorg. Chem.* **1978**, *17*, 189.
(27) Spivack, B.; Dori, Z. *J. Chem. Soc., Chem. Commun.* **1973**, 909.

Table 3. ^{183}W NMR Data for $Li_{10}\Delta_1$- and Li_{10} Δ_2-$[(PW_{11}O_{39})_2(Mo_4S_4O_4(OH)_2]$ in Water

isomer	chemical shift/ppm ($^2J_{P-W}$/Hz)
$Li_{10}\Delta_1$-$[(PW_{11}O_{39})_2(Mo_4S_4O_4(OH)_2]^{10-}$	−101.00[a]; −103.60[a]; −118.60 (0.91); −122.2[a]; −123.90 (2.0); −132.40[a]; −137.70[a]; −148.60[a]; −148. 95[a]; −159.20 (0.8)
$Li_{10}\Delta_2$-$[(PW_{11}O_{39})_2(Mo_4S_4O_4(OH)_2]]^{10-}$	−101.00[a];−105.85[a]; −118.10 (0.95); −120.90[a]; −126.60 (1.0); −130.85[a]; −137.40[a]; −143.05 (0.85); −149.40[a]; −149.55[a]; −150.60[a]

[a] The P−W coupling constant is not observed.

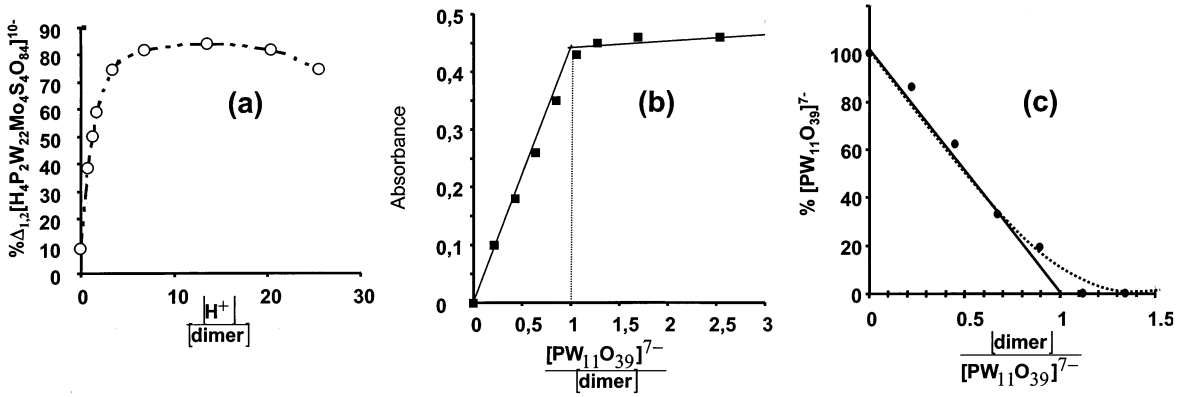

Figure 11. Spectroscopic titrations in water: (a) H^+ titration of $\{Mo_2\}/[PW_{11}] = 1$ solution monitored by UV−vis spectroscopy; (b) $[PW_{11}O_{39}]^{7-}$ titration of $[Mo_2O_2S_2]^{2+}$ with fixed ratio $[H^+]/[Mo_2O_2S_2]^{2+} = 4$, monitored by UV−vis; (c) $[Mo_2O_2S_2]^{2+}$ titration of $[PW_{11}O_{39}]^{7-}$ monitored by ^{31}P NMR with $[H^+]/\{Mo_2O_2S_2\} = 4$.

Table 4. UV−Vis Data for 0.00182 mol·L^{-1} $[Mo_2O_2S_2]$ Solutions

	medium	pH	peak/nm (ϵ/mol^{-1}.L.cm^{-1})
$[Mo_{10}]$	[NaCl] 0.05 mol·L^{-1}	3.5	340 (1785) 280 (7375) 223 (22 160)
$[Mo_2O_2S_2]^{2+}$	[NaCl] 0.05 mol·L^{-1}	1.77	370 (1825) 300sh (4340) 280 (5480) 225 (17 700)
	[$HClO_4$] 2 mol·L^{-1}		370 (1770) 300sh (4165) 280 (5165) 225 (16 600)

taneously the two isomers cisoid and transoid under equilibrium conditions.

Conclusions

The reliable synthetic procedure we developed for the formation of the title compound, $\Delta_{1,2}$-$[(PW_{11}O_{39})_2(Mo_4S_4O_4(OH_2)_2)]^{10-}$, is general and could be extrapolated to other polyvacant polyoxoanions. Among the parameters of synthesis, the control of the pH appears crucial to obtain a high yield. The reaction of the monovacant α-$[PW_{11}O_{39}]^{7-}$ anion toward the acidic oxothiocation leads to a "sandwich-like" compound, enclosing a central unusual cluster $\{H_4Mo_4S_4O_6\}$. The isomerization process between cisoid and transoid was evidenced by ^{31}P and ^{183}W NMR, but these techniques, although supported by the single-crystal X-ray diffraction method, do not allow discrimination between the arrangement of the syn−syn (C_2 symmetry) and anti−anti conformations (C_s symmetry). At this level, theoretical calculations should supply additional information to determine the most probable arrangement.

Supporting Information Available: Crystallographic data in CIF format. This material is available free of charge via the Internet at http://pubs.acs.org.

IC026191J